# POLYSTYRENE PARTICLES AND MAMMALIAN CELLS MOTION BEHAVIOUR ON DIFFERENT SURFACES

**M Mohamad Shahimin[1,*], S A Z Murad[1], N M B Perney[2], N Hanley[2,3], J S Wilkinson[4,5] and T Melvin[4,5]**

[1]School of Microelectronic Engineering, University Malaysia Perlis, Malaysia

[2]Endocrinology & Diabetes, Manchester Academic Health Science Centre, University of Manchester, UK

[3]Centre for Human Development, Stem Cells and Regeneration, Division of Human Genetics, School of Medicine, University of Southampton, UK

[4]Optoelectronics Research Centre, University of Southampton, UK

[5]School of Electronics & Computer Science, University of Southampton, UK

Email: 1mukhzeer@unimap.edu.my

***ABSTRACT***

*The stochastic motion behaviour of polystyrene particles and teratocarcinoma cells on plain and functionalised surfaces is investigated and analysed. The solution of 1 x 106 particles/cells per ml concentration is pipetted into a reservoir and images are captured and analysed using an in-house written software. A theoretical model was used to predict the motion and compared to the experimental results. The conditions and limitations to allow particles and cells to move freely in stochastic motion on surface are discussed in this paper. PEG functionalisation of the glass surface was found to improve the particles and cells mobility, on average 26%. Analysis technique proposed in this paper demonstrates that size distribution of different cell line can be determined. The results are presented in light of the potential application of the observed motion on functionalised surfaces for lab-on-a-chip devices, especially for adherent biological cells applications.*

***KEYWORDS****: Stochastic, Brownian motion, polystyrene particle, biological cells, PEG, surface functionalisation*

## 1.0 INTRODUCTION

The use of optical trapping and planar optics as a versatile and non-contact tool is becoming a ubiquitous trend within diverse technological disciplines for precise particle and cell handling. Over the years, these optical trapping and planar manipulation techniques were found to apply over a wide range of particle types, including particles as diverse as atoms [1], molecules [2], microscopic dielectric particles and biological cells [3-5].

According to works by [3-5], optical trapping and propulsion on a channel waveguide device have shown its potential to sort and discriminate biological cells of different sizes and refractive index. This has a significant clinical advantage for biological applications where optical selection has never been thoroughly developed. Furthermore the channel waveguide configuration permits integration with microsystems for a lab-on-a-chip device. However, current systems [3-5] only works with non-adherent cells, rendering less applicability to adherent cells; by far the most common cell phenotype [6]. Adherent cells express abundant adhesion proteins on their membranes that provide a structural link between their cytoskeleton and extracellular surfaces [6]. Hence, a fundamental understanding of how surface properties might affect the overall motion behaviour becomes crucial to the design of these integrated devices for adherent cells application.

The project investigated stochastic motion of polystyrene particles (Polysciences Inc, 15μm and 20μm in diameter) and adherent mammalian eukaryotic cells, teratocarcinoma (Southampton General Hospital). Teratocarcinoma cells are an adherent germ cell tumour [7, 8]. There are two teratocarcinoma cell lines used in this project, namely TERA1 (a stable, undifferentiated cell line) and NT2 (prone to cell differentiation). The continuous stochastic motion of particles and cells, suspended in various liquid media and on two different surfaces (plain and PEG functionalised) are investigated in this paper. Different aspects such as particle size and functionalisation of surfaces are then examined with relation to their statistically tabulated signatory motion on the surface.

## 2.0 TECHNIQUES AND MATERIALS

### 2.1 Image Acquisition

Stochastic motion of polystyrene particles and teratocarcinoma cells was investigated through a series of images that were analysed using in-house written programs. In order to capture these images, a Nikon optical stereomicroscope (Universal Epi-illuminator 10), equipped with a cooled CCD camera (QImaging, Monochrome Retiga 1300) was used to observe the particles and cells.

The solution containing particles or cells was pipetted into a reservoir (CoverWell, Z379077, Sigma Aldrich) placed on a soda-lime glass slide positioned using a vacuum holder (Thorlabs, HWV001), as depicted in Figure 1. The microscope was adjusted in a way that it only focused on the surface of the glass slide, to ensure that only particles/cells close to the surface were observed.

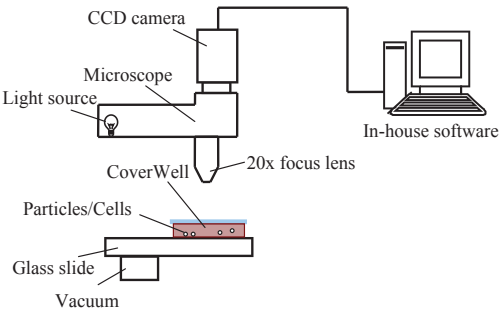


**Figure 1** Experimental set up for monitoring particle and cell movements

## 2.2 Image Analysis

Typically up to 10,000 images were taken for each stochastic motion experiment. Each of these images covers 30 to 90 particles or cells (for a concentration of 1 x $10^6$ particles/cells per ml) using the 20x objective lens. The experiments were repeated at least three times which makes every data point presented an average of up to 270 measurements for particles and up to 400 for cells (due to more experimental cycles). Solid particles such as polystyrene particles reflect more light and hence require a shorter integration time compared to the mostly transparent, teratocarcinoma cells. Hence, the frame rate has to take into consideration the integration time of the camera and also the level of binning required of each object.

All the images are presented by one dimensional hexadecimal matrix. Images are loaded into the program and translated into two dimensional matrices for image analysis. The output is presented in black and white images for example as illustrated in Figure 2 a). A threshold level is made in order to identify particles and distinguish the background value to be 255 (black) and the particle to be 0 (pure white) as indicated in Figure 2 b). The threshold value is taken to be:

$$T_{pixel} = \langle P_{pixval} \rangle + (2 \times \sigma(P_{pixval})) \quad (1)$$

where $T_{pixel}$ is the pixel threshold and $P_{pixval}$ is the pixel value. Equation (1) is used for determining the pixel threshold and hence detecting particles and cells. The distance travelled by each particle/cell, for each frame, is tabulated for subsequent graphical representations.

### 2.3 Error Estimation

Errors occurring during the data collection and analysis of the stochastic motion are inevitable. Most of the errors usually originated from a physical limitation such as the microscope illumination brightness and camera detector sensitivity. Three types of error are described in this section; random, systematic and dynamic errors.

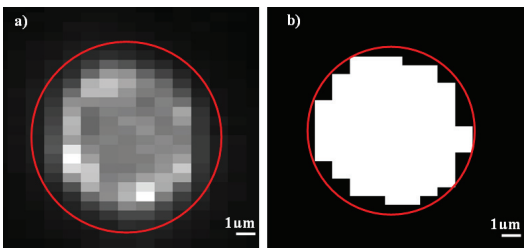


**Figure 2** Image of a 10µm polystyrene particle a) prior and b) after the thresholding process

One of the major contributors to errors during the data collection process is from the camera noise. This random error originates from the statistical fluctuation in the number of photons detected by the camera. Such fluctuations still exist even in an ideal condition, due to the nature of the microscope illumination. In order to estimate the error from camera noise, the variation of size from one frame to another for a specific particle is tabulated. Their corresponding error in determining their exact position for each frame is calculated and averaged. Table 1 shows the errors from camera noise for a specific particle size and cell.

**Table 1** Tabulation of polystyrene particles and cells size distribution and their corresponding errors measurements. Note that the measured diameter and size deviation for the particles were provided by the manufacturer. Diameter and size distribution for the cells were measured using Zeiss Axio Observer Z1 microscope

| **Particles/ Cells** | **Measured diameter (μm)** | **Size standard deviation (μm)** | **Error from camera noise (x $10^{-3}$μm)** | **Error from thresholding process (x $10^{-3}$μm)** |
|---|---|---|---|---|
| 20 | 20.99 | 1.24 | 1.7 | 2.2 |
| 15 | 16 | 2.56 | 2.2 | 3.1 |
| NT2 | 18.91 | 3.12 | 6.9 | 21.7 |
| TERA1 | 17.73 | 2.46 | 5.4 | 24.4 |

The thresholding process during the data analysis and the limitation arising from the camera detector can cause pixel biasing in the image identification; this results in an ill-defined boundary as shown in Figure 2a). This is a typical systematic error when capturing a 3D object in a 2D image. Error due to the thresholding process is calculated by comparing the size of the threshold image and the measured size for each particle. The bias in determining the exact position of the particle/cell is tabulated and averaged as shown in Table 1.

Apart from that, there are several other sources of error. A phenomenon such as drifting is common when securing particles or cells in solution in a reservoir such as CoverWell. An imbalance of water pressure due to uneven surfaces, the existence of air bubbles or thermal expansion arising from illumination can all be possible factors that cause drifting. Furthermore, there is also vibration from the laboratory environment to consider and also the measurement of stochastic motion in 2D (despite the fact that the particles and cells are moving in 3D). However such dynamic errors can be minimised through a detrending analysis [9], which is a computational correction for global error. This technique however has the possibility of reducing the distance travelled due to stochastic motion. Errors from drifting, for instance, can also be detected just by the monitoring of live data from the microscope by an experienced observer. Corrective action such as levelling the glass slide or switching off the microscope light for a while to prevent overheating will minimise the drift effect.

### 2.4 PEG Surface Functionalisation

Polyethylene glycol (PEG) based surface passivation techniques have been demonstrated to prevent cell adhesion [10-14] due to the properties of the oligomer. The oligomer of PEG is hydrophilic and non-structure-forming which act against the association of proteins. Adhesion due to the dominance of van der Waals force can be reduced by physically increasing the distance between the particles or cells and the surface. OH groups are created on the glass slide surface to be reacted with the silane group in the PEG chain. A spacer is included between the PEG chain and silane group as a steric protection against unwanted side reactions. The PEG layer used in this project is fabricated by cleaning the glass slide in a weak piranha solution; which is a solution of $NH_4OH$, $H_2O_2$, and DI water in a ratio of 1:1:5. This cleaning process creates the OH group on the glass surface. After washing with deionised water and drying, the glass slide is soaked in derivatisation solution made of 4% PEG-silane (Gelest – SIM6492.7) in toluene. The glass slide is left for 24 hours before cleaning consecutively with anhydrous toluene and ethanol. The glass slide is then cured for 30 minutes at 100°C in an oven.

## 3.0 RESULTS AND DISCUSSION

Stochastic motion investigations were carried out using the polystyrene particles and two types of teratocarcinoma cells; NT2 and TERA1. Two controllable factors that can influence stochastic motion are viscosity and temperature. Viscosity was maintained by using samples from the same particle solution for each data acquisition run. The fluctuation in the temperature was minimised through the restriction of the microscope illumination to avoid heating the solution in a temperature moderated laboratory.

### 3.1 Motion of polystyrene particles on functionalised surface

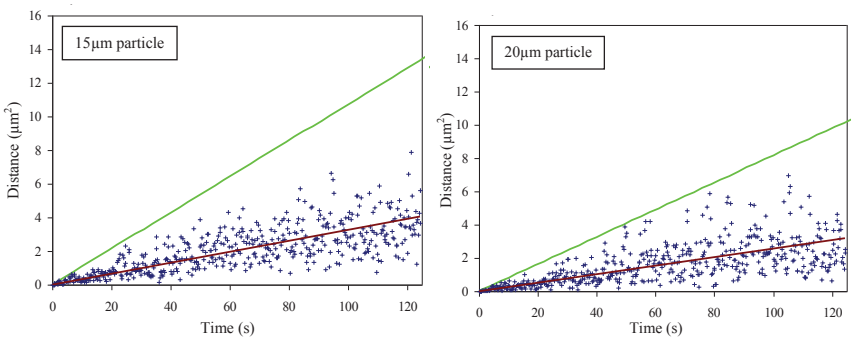


a) b)

**Figure 3** The distance travelled (squared) from one frame to a subsequent frame by particles of different sizes on a plain glass surface in water. The theoretical data (—), experimental data (+) and linear best fit line for the experimental data (—) are plotted for each particle size

The theoretical representation of the stochastic motion, as derived in [15-18], can be interpreted in practice as,

$$<r^2> = Ln_s(t) \tag{2}$$

which means that the mean square distance, $<r^2>$, of any particle is equal to the number of steps taken, $n_s$, of a specific time, $t$, multiplied by the length, $L$, of each step. The distance travelled was tabulated and a graphical representation of the particle motion is illustrated in Figure 3.

Figure 3 illustrates that the data points sometimes jumps or falls drastically from one frame to another resulting a 'ripple' motion in the measurements. This type of particle motion is non-physical and is most likely to arise from errors such as from the thresholding process, as described in Section 2.3. The best fit linear line, included in each graph, is regarded as the true representation of the particle motion. The slope of the linear fit line reflects the dependency on the size of the particle and can be compared with the theoretical plot [19, 20], which included in the graphs. A reduction in gradient, of 69% in average, was observed for the 15μm and 20μm particle sizes.

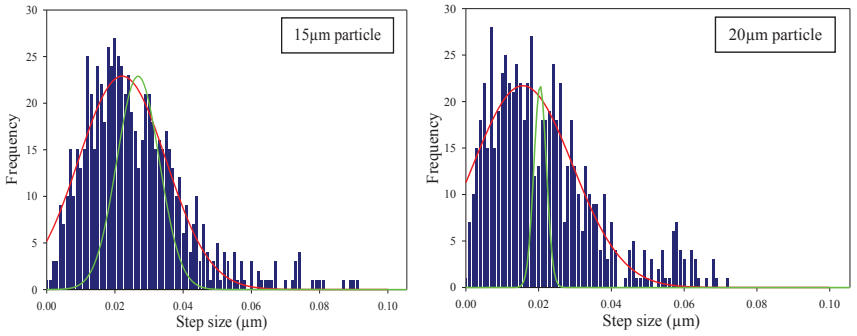


**Figure 4** The histograms of the step size taken to travel from one frame to a subsequent frame by a) 15µm and b) 20 µm particles a plain glass surface in water. The Gaussian best fit line (—) is plotted for each experimental data (■) alongside the theoretical model (—)

Data presented in Figure 3 is re-plotted in a histogram format by compiling the frequency of distance travelled between each frame. Figure 4 shows a series of histograms for all polystyrene particles under consideration.

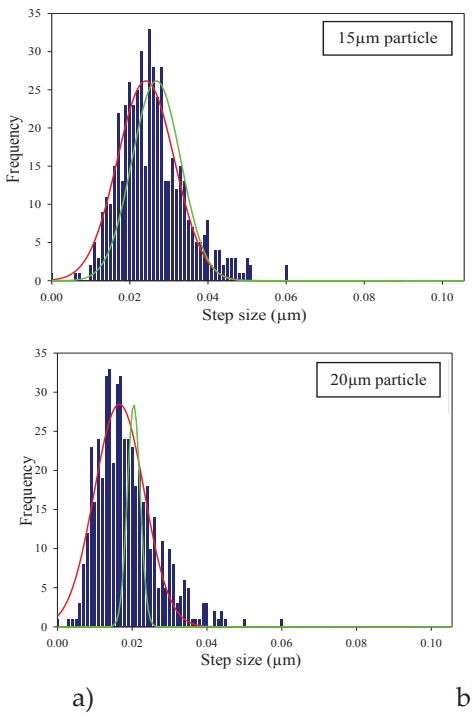


**Figure 5** The histograms of the step size taken to travel from one frame to a subsequent frame by a) 15µm and b) 20 µm particles a PEG functionalised glass surface in water.

All histogram plots are fitted with a Gaussian profile and their corresponding theoretical Gaussian profile. The theoretical projection of distance travelled by the particles was calculated (refer to Section 2.3) from the measured particle diameter and the corresponding size distribution as listed in Table 1. The Gaussian width or full width half maximum (FWHM) was calculated from equation,

$$\mathrm{FWHM} = e^{-x^2/(2\sigma^2)} = 2\sqrt{2\ln 2}\sigma \tag{2}$$

where $\sigma$ denotes the standard deviation. The peak frequency of the Gaussian profile was made equal to the experimental Gaussian plot for comparison.

The peak value of the Gaussian fitted line on the experimental data is equivalent to the average particle size. The width of the Gaussian profile corresponds to the size distribution of the particle as well as the errors in the data acquisition/analysis and the interaction between the particle and the surface. Inconsistency between the theoretical and experimentally observed stochastic motion especially for the large size particles can be explained from different aspects. Van der Waals force between the surface and the particles, indicates that the force is proportional to the particle size and inversely proportional to the separation distance. Furthermore the gravitational force is also proportional to particle size, hence increasing the attractive force via the reduction of separation distance for larger particles.

Reduction in separation distance also changes the boundary condition for the stochastic motion theory, as explained in [21-24]. The drag force in this case is expected to increase as the effective local viscosity is increased. Hence large particles (15μm and 20μm) were observed to move significantly more slowly than predicted by the theory. Note that the stochastic motion theory considered here assumed that the mass of the particle is small and that the particle is moving in 2D in an unbounded medium. Hence, these factors introduce more error in the image analysis and are consequently translated into a wider width of the Gaussian profile.

### 3.2 Motion of polystyrene particles on functionalised surface

Histograms of particle motion, as shown in Figure 5 illustrate an overall improvement in the stochastic motion from the maximum frequency and

the width of the Gaussian profile extracted for all particle sizes. The maximum frequency of the step size taken, within the frame rate, is increased on average by 20% while the width decreased by 49% for large (15μm and 20μm) particles. $R^2$, which is known as the correlation of determination, is the statistical evaluation of the goodness of fit of a model vis-à-vis experimental data. The $R^2$ value for the histograms in Figure 5, on average, is 0.92. In comparison, the R2 value for histograms in Figure 4 is 0.89. The frequency increment, narrower width and higher $R^2$ value indicate that PEG functionalisation improves the stochastic motion of particles on a surface by minimising the effect of the van der Waals and the drag force that act against the motion.

### 3.3 Motion of single cells

Teratocarcinoma cells were prepared for the stochastic experiments by trypsinisation process and re-suspended in a fresh DMEM solution (with phenol red and 10% serum) [25]. The cells were pipetted on the surface of the glass slide and the motion of each cell was analysed from the frames taken. More frames were taken for this experiment (up to 10,000 frames for a single experimental cycle) particularly targeted for better cell motion detection and to increase the probability of detecting each cell. The cell solution is changed every 1 hour to maintain the same cell condition for all data acquired. All experimental data are compared with the theoretical model [21-24].

Figure 6 illustrates the distance travelled by the TERA1 and NT2 cells respectively. Note that after 125 seconds, the cells on average moved about 2.8μm. At this rate, the motion of the cell matches the motion of a 20μm polystyrene particle moving on a plain surface. The experimental peak value of the Gaussian best fit line matched (within 10%) the theoretical peak. However, the widths of the experimental histogram are observed to be 40% to 50% wider than the theoretical model.

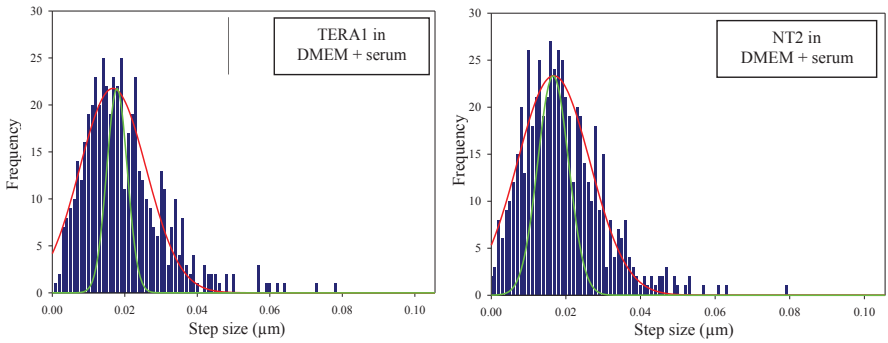


a) b)

**Figure 6** The histograms of the step size taken to travel from one frame to a subsequent frame by a) TERA1 and b) NT2 cell on a PEG functionalised glass surface in DMEM with serum.

### 3.4 Motion of a group of cells

Analysing teratocarcinoma cells individually reveals properties specific to the cell stage, surface characteristics and cell size. Analysing the whole population of cells has the benefit of reducing errors within each single data point. Figure 7 b) illustrates the histogram of the step size taken in each frame for NT2 cells. Comparing this graph to Figure 7 a) shows that the distribution of step sizes of NT2 cells is broader than for TERA1 cells. As the experimental setup and the data collection process for both cell types was the same, a wider histogram width for NT2 might indicate a larger size distribution. This agrees with the measurements tabulated in Table 1 which shows a wider standard deviation for NT2 cells. Both cells have approximately the same average size; 19μm for NT2 and 18μm for TERA1 cells as estimated from the Gaussian best fit profile and these values concur with the average cell size measurements using the microscope. The width of the theoretical Gaussian profile is still slightly smaller than the experimental value for both cells. Width difference for TERA1 is about 29% and for NT2 is 34%. The $R^2$ value for the Gaussian fit in Figure 7 is 0.94 and corresponds to the reduced variance in the plot of the distance travelled. This is an 8% improvement compared to Gaussian fit for single cells.

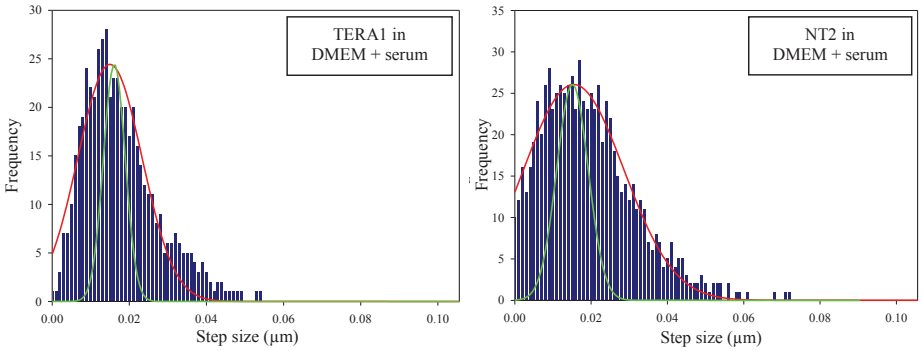


a) b)

**Figure 7** The histograms of the step size taken to travel from one frame to a subsequent frame by a group of a) TERA1 and b) NT2 cells on a PEG functionalised glass surface in DMEM with serum.

## 4.0 CONCLUSION

The results presented in this paper show the investigation of stochastic motion for particles and cells and the limitation of their mobility. It was found that PEG functionalisation of the glass surface improves the particles and cells mobility, on average 26%. Analysis of single and multiple cells shows that individual errors can be eliminated and size distribution of cells can be determined from their stochastic motion signature. Thus, using the experimental setup, manipulation of particles and cells will benefit from the PEG surface functionalisation; especially when experimenting with the naturally adherent biological cells.

## 5.0 ACKNOWLEDGMENT

The authors thank Dr S Brooks, KL Wright and Prof. Dr DI Wilson (Centre for Human Development) for provision of training to MMS and support for the cell culture, and BBSRC (BBD0146702), FRGS (9003-00235) and STG (9001-00256) are acknowledged for the funding used for this investigation.

## 6.0 REFERENCES

M. I. Dykman, "Statistical physics: Swirled by light," *Nature*, vol. 461, pp. 1226-1226, 2009.

P. Meystre, "From micromasers to atom optics and back," *Laser Physics*, vol. 15, pp. 99-106, 2005.

A. H. J. Yang, *et al.*, "Optical manipulation of nanoparticles and biomolecules in sub-wavelength slot waveguides," *Nature,* vol. 457, pp. 71-75, 2009.

S. Gaugiran, *et al.*, "Optical manipulation of microparticles and cells on silicon nitride waveguides," *Optics Express,* vol. 13, pp. 6956-6963, 2005.

M. M. Shahimin, *et al.*, "Optical propulsion of mammalian eukaryotic cells on an integrated channel waveguide," in *Microfluidics, BioMEMS, and Medical Microsystems IX, January 23, 2011 - January 25, 2011*, San Francisco, CA, United states, 2011.

C. Jensen-McMullin, *et al.*, "A microfluidic assembly line for adherent cell assays," in *2005 3rd IEEE/EMBS Special Topic Conference on Microtechnology in Medicine and Biology, May 12, 2005 - May 15, 2005*, Oahu, HI, United states, 2005, pp. 34-37.

T. P. Zwaka and J. A. Thomson, "A germ cell origin of embryonic stem cells?," *Journal of Development,* vol. 132, pp. 227-233, January 15, 2005 2005.

M. Conti and L. Giudice, "From stem cells to germ cells and back again," *Nature Medicine,* vol. 14, pp. 1188-1190, 2008.

C. Heneghan and G. McDarby, "Establishing the relation between detrended fluctuation analysis and power spectral density analysis for stochastic processes," *Physical Review E,* vol. 62, p. 6103, 2000.

A. Wolter, *et al.*, "Preparation and characterization of functional poly(ethylene glycol) surfaces for the use of antibody microarrays," *Analytical Chemistry,* vol. 79, p. 4529, 2007.

S. Mandal, *et al.*, "Cytophobic surface modification of microfluidic arrays for in situ parallel peptide synthesis and cell adhesion assays," *Biotechnology Progress,* vol. 23, p. 972, 2007.

G. M. Harbers, *et al.*, "Functionalized poly(ethylene glycol)-based bioassay surface chemistry that facilitates bio-immobilization and inhibits nonspecific protein, bacterial, and mammalian cell adhesion," *Chemistry of Materials,* vol. 19, pp. 4405-4414, 2007.

K. C. Popat and T. A. Desai, "Poly(ethylene glycol) interfaces: an approach for enhanced performance of microfluidic systems," *Biosensors & Bioelectronics,* vol. 19, pp. 1037-44, 2004.

E. Tziampazis, *et al.*, "PEG-variant biomaterials as selectively adhesive protein templates: Model surfaces for controlled cell adhesion and migration," *Biomaterials,* vol. 21, pp. 511-520, 2000.

J. Dongdong, *et al.*, "The time, size, viscosity, and temperature dependence of the Brownian motion of polystyrene microspheres," *American Journal of Physics,* vol. 75, p. 111, 2007.

S. Sudo, *et al.*, "Quick and easy measurement of particle size of Brownian particles and plankton in water using a self-mixing laser," *Optics Express,* vol. 14, 2006.

R. V. Durand and C. Franck, "Investigation of apparent correlated motion of Brownian particles," *Physical Review E,* vol. 56, p. 1998, 1997.

J. l. P. Webb, "Einstein and Brownian motion-a student project," *Physics Education,* vol. 15, p. 116, 1980.

A. Einstein, "The motion of small particles suspended in liquid at rest required by the molecular kinetic theory of heat," *Annalen der Physik,* vol. 17, pp. 549-560, 1905.

A. Einstein, "The theory of Brownian motion," *Annalen der Physik,* vol. 19, pp. 371-381, 1906.

H. Jensenius and G. Zocchi, "Measuring the spring constant of a single polymer chain," *Physical Review Letters,* vol. 79, p. 5030, 1997.

J. P. Hole, "The Control of Gold and latex Particles on Optical Waveguide," PhD thesis, Optoelectronics Research Centre, University of Southampton, Southampton, 2005.

N. A. Frej and D. C. Prieve, "Hindered diffusion of a single sphere very near a wall in a nonuniform force field," *Journal of Chemical Physics,* vol. 98, pp. 7552-64, 1993.

B. Cichocki, *et al.*, "Friction and mobility for colloidal spheres in Stokes flow near a boundary: The multipole method and applications," *Journal of Chemical Physics,* vol. 112, pp. 2548-2561, 2000.

M. M. Shahimin, "Propulsion of polymer particles on ceasium ion-exchanged channel waveguides for stem cell sorting applications," PhD Thesis, School of Electronics and Computer Sciences, University of Southampton, Southampton, 2009.